Polarization-dependent formation of biexcitons in (Zn,Cd)Se/ZnSe quantum wells

R. Spiegel, G. Bacher, and A. Forchel
Technische Physik, Universität Würzburg, Am Hubland, D-97074 Würzburg, Germany

B. Jobst,* D. Hommel,* and G. Landwehr
Experimentelle Physik III, Universität Würzburg, Am Hubland, D-97074 Würzburg, Germany
(Received 17 October 1996)

The dynamics of biexciton formation and the spin-relaxation process of excitons in (Zn,Cd)Se/ZnSe quantum wells are investigated systematically using time-resolved photoluminescence spectroscopy. Excitons with well-defined spin orientation were created using linearly or circularly polarized light, respectively, while the energy of the exciting laser pulse was tuned to the transition of the ground state of the heavy-hole exciton. For linearly polarized excitation, the rise time of the biexciton luminescence signal directly reflects the biexciton formation coefficient. For circularly polarized laser pulses, a strong increase of the rise time of the biexciton photoluminescence signal is observed, which is attributed to the necessity of an exciton spin-flip process in the case of circular polarization in order to form biexcitons. The experimental data were evaluated numerically by using a system of rate equations. Generating resonantly localized excitons, we obtain a biexciton-formation coefficient of about 5.2×10^{-11} cm^2/ps and an exciton spin-flip time of 70 ps. Increasing the excitation energy (i.e., creating more mobile excitons), we obtain a drastically reduced spin-flip time, indicating that exchange interaction is the leading exciton spin-relaxation mechanism. [S0163-1829(97)02516-2]

I. INTRODUCTION

Excitons in wide-band-gap II-VI quantum-well structures are characterized by an enhanced exciton binding energy as compared to common III-V compounds.[1] High exciton binding energies support the formation of biexcitons (excitonic molecules) in these wide-band-gap II-VI materials.[2–6] Typical biexciton binding energies in the range between 6 and 10 meV were reported for a variety of ZnSe-based quantum wells.[3,7,8] In order to understand quantitatively the biexciton binding energy, Puls *et al.* have shown that localization of biexcitons, e.g., on alloy disorder in ternary (Zn,Cd)Se/ZnSe quantum wells has to be taken into account, resulting in a higher stability of the biexciton complex.[9,10] Concerning the dynamics of biexcitons, many controversial results were reported about the biexciton lifetime. Yamada *et al.*[3] have measured a biexciton lifetime of 6 ps in (Zn,Cd)Se/Zn(Se,S) quantum wells, much shorter than the exciton lifetime and in contrast to theoretical predictions of a strongly suppressed decay rate of biexcitons compared to excitons.[11] Other authors determined the biexciton lifetime in (Zn,Cd)Se/ZnSe quantum wells to about 130 ps,[5,9] while in GaAs-based quantum wells the biexciton lifetime amounts to about half of the exciton lifetime.[12,13] On the other hand, detailed investigations of the biexciton formation process in II-VI quantum wells are still lacking.

As a biexciton involves two excitons with opposite spin orientations, the basic mechanism of the spin relaxation process of excitons in II-VI quantum wells is of fundamental interest for a quantitative understanding of the biexciton formation process. However, up to now, most experimental investigations concerning spin-relaxation processes are limited to GaAs quantum wells.[14–16] Damen *et al.* reported an electron-spin-relaxation time of about 50 ps and an instantaneous spin relaxation for the heavy holes,[17] while Bar-Ad and Bar-Joseph determined the electron-spin-relaxation time to about 120 ps and the heavy-hole spin-relaxation time to about 50 ps in intrinsic GaAs quantum wells.[16] In contrast, Muñoz *et al.*[14] have considered the simultaneous spin flip of electrons and holes in addition to consecutive spin-flip processes. In agreement with theoretical predictions,[18,19] they have shown that the long-range exchange interaction is the leading exciton-spin-relaxation mechanism in intrinsic quantum wells changing the exciton spin, e.g., from a $|+1\rangle$ into a $|-1\rangle$ (or vice versa) state.[18,19] Also, they have found that at low temperatures excitonic localization strongly affects this mechanism, resulting in a reduced spin-flip rate. On the other hand, data related to spin-relaxation processes in II-VI quantum wells are limited to investigations of the spin-flip mechanism of electrons in diluted-magnetic semiconductor quantum wells based on the $Cd_xMn_{1-x}Te$ material system,[20] where electron-spin scattering is discussed as a consequence of spin-spin exchange interaction with the magnetic ions.

In this paper we present a systematic study of the biexciton formation process in (Zn,Cd)Se/ZnSe quantum wells. Exciting resonantly excitons with either linearly or circularly polarized laser pulses, an exciton system with a well-defined spin orientation is generated. As the biexciton involves excitons with opposite spin orientations, the onset of the biexciton luminescence signal is used as a monitor for the spin-flip process of excitons for circularly polarized laser pulses and for the biexciton formation process in the case of linearly polarized excitation, respectively. By varying the energy and the density of the exciting laser pulse, we are able to determine the dominating spin-flip mechanism of excitons in (Zn,Cd)Se/ZnSe quantum wells.

II. EXPERIMENTAL DETAILS

The $(Zn_{0.88},Cd_{0.12})Se/ZnSe$ quantum-well heterostructure under investigation was grown by molecular-beam epi-

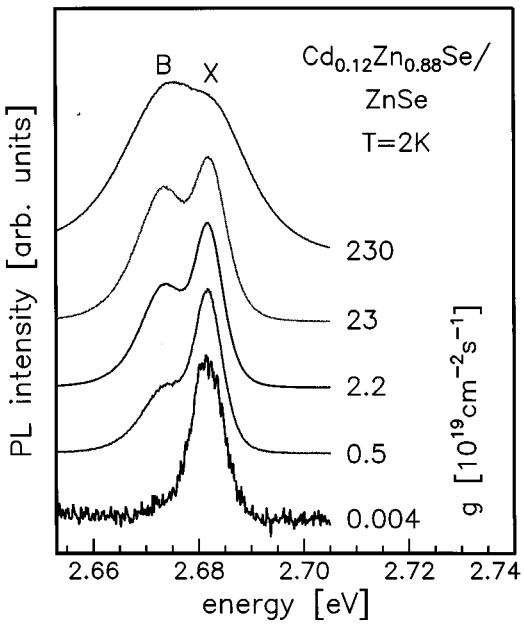

FIG. 1. Normalized PL intensity at $T=2$ K of a (Zn,Cd)Se/ZnSe quantum well for different cw excitation densities.

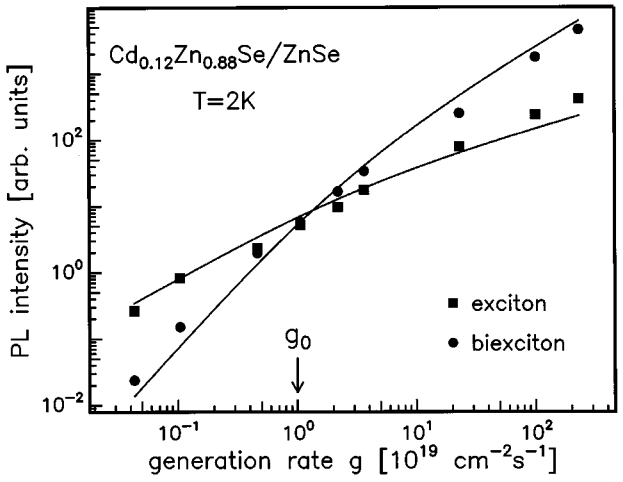

FIG. 2. Spectrally integrated PL intensities of the exciton (X) and biexciton (B) signal of a (Zn,Cd)Se/ZnSe quantum well as a function of the generation rate. The solid lines represent the fits according to Eq. (1).

taxy on a (100)-oriented undoped GaAs substrate and a 200-nm GaAs buffer layer at a growth temperature of 315 °C. The $L_z=5$ nm quantum well layer is embedded between a 20-nm ZnSe top barrier layer and a 70-nm ZnSe buffer layer. The extension of the complete structure is below the critical thickness and is therefore fully strained with the in-plane lattice constant of the GaAs substrate. In order to guarantee a homogeneous excitation, a mesa structure with an extension of 50 μm, i.e., smaller than the exciting laser focus, was fabricated using a combination of electron-beam lithography and wet chemical etching with a bromine in ethyleneglycole solution.[21]

The time-resolved photoluminescence (PL) experiments have been performed at a temperature of 2 K using a frequency-doubled mode-locked Ti-sapphire laser with a pulse width of 1.5 ps and a repetition rate of 82 MHz. The exciting light was circularly polarized using a $\lambda/4$ plate and linearly polarized with a polarization filter, respectively. The luminescence signal was dispersed by a 0.32-m spectrometer with a spectral resolution better than 0.2 nm and detected by a synchroscan streak camera followed by a charge coupled device array, providing an overall time resolution of about 5 ps. For comparison, cw measurements have been performed using the 363.8-nm line of an argon-ion laser for the excitation and a charge coupled device camera for the detection.

III. RESULTS AND DISCUSSION

A. Exciton and biexciton recombination

In Fig. 1 a set of time-integrated spectra of the (Zn,Cd)Se/ZnSe quantum well at T=2 K is shown for cw laser excitation and excitation densities ranging from 0.02 W/cm^2 to 1.15 kW/cm^2, which correspond to exciton generation rates between 4.0×10^{16} and 2.3×10^{21} cm^{-2} s^{-1}. The spectra are normalized to the peak exciton intensity in order to compare the line shape. Below a generation rate of about 4×10^{17} cm^{-2} s^{-1}, the spectrum consists of a single line that is attributed to the radiative recombination of the heavy-hole exciton. For higher excitation intensities, a second peak appears energetically below the exciton luminescence, which increases in intensity superlinearly with the excitation density. As impurity or defect related luminescence is expected to saturate at high excitation powers, the low-energy peak is attributed to the recombination of biexcitons.[2–5,7,9,12,22] The energetic distance of 9 meV between the exciton and the biexciton emission peak, which is controlled by both the biexciton binding energy and the localization energies of excitons and biexcitons, respectively,[9] is in good agreement with literature data for ZnSe-based quantum wells.[3,4,6,9]

For an estimate of the relative intensities of the exciton and the biexciton luminescence, the exciton and biexciton components of the photoluminescence spectra are separated by using a double Gaussian function.[10] The theory predicts a Boltzmann distribution for the exciton and a reverse Boltzmann distribution for the biexciton line shape.[8] However, due to the low temperature in our experiments ($T=2$ K), the thermal energy kT is small compared to the inhomogeneous broadening of the exciton and the biexciton luminescence spectrum. In addition, excitons and biexcitons are even localized in this temperature range.[10] Thus the fit by a double Gaussian line shape is expected to be a good approximation. In Fig. 2 the spectrally integrated intensities of the exciton and biexciton lines are plotted versus the exciton generation rate. In the low-density limit, the biexciton intensity increases superlinearly, while a linear growth of the exciton intensity is observed. In contrast, for high excitation densities, a slower rise of both intensities occurs. For all laser powers, however, the biexciton intensity depends quadratically on the exciton intensity.

The rate equations for a system of excitons n_X and biexcitons n_B are given by Kim *et al.*[12] with the steady-state solutions

$$n_X \propto \left[\left(1+\frac{g}{g_0}\right)^{0.5}-1\right], \quad n_B \propto \left[\left(1+\frac{g}{g_0}\right)^{0.5}-1\right]^2, \quad (1)$$

where g is the continuous generation rate and g_0 is a characteristic generation rate separating the exciton-dominant region from the biexciton-dominant region.[22] In Fig. 2, $n_X(g)$ and $n_B(g)$ according to Eq. (1) are shown as solid lines. Good agreement between the experimental data and the theoretical model is obtained using a characteristic generation rate $g_0 = 1 \times 10^{19}$ cm^{-2} s^{-1}. As can be seen from Fig. 2, for generation rates less than g_0 the exciton population is prevalent, while for generation rates greater than g_0 the biexciton emission dominates the photoluminescence spectrum.

B. Biexciton formation dynamics after linearly and circularly polarized excitation

While cw measurements only yield information about the quasiequilibrium distribution between excitons and biexcitons, time-resolved measurements reveal the dynamics of the biexciton recombination and formation process. The decay time of the exciton signal was found to be 48 ps, while for biexcitons a time constant of 65 ps was measured. In the case of a thermodynamic equilibrium (i.e., the interconversion time between excitons and biexcitons is much shorter than the recombination lifetimes) the biexciton decay time is expected to be half of the exciton decay time.[12] However, in the (Cd,Zn)Se/ZnSe system under investigation, the biexciton formation time is almost comparable to the lifetimes (see below). In addition, due to the high biexciton binding energy and the low temperature of 2 K, the thermal dissociation of biexcitons into two excitons is negligible. This may possibly account for the enhanced decay time of the biexciton compared to the exciton observed in our experiments. It should additionally be mentioned that calculations of Citrin[11] within the excitonic molecule model have shown that the radiative recombination rate of biexcitons can indeed be even smaller than for excitons, in agreement with our data.

To analyze the biexciton formation dynamics, the wavelength of the exciting laser was tuned to the excitonic absorption peak, thus creating excitons resonantly, i.e., avoiding the generation of free electrons and holes. Either linearly or circularly polarized laser light was used in order to obtain a well-defined initial exciton-spin state. In direct-gap semiconductors the component of the total angular momentum of the exciton in the z direction can have the values $|\pm\frac{1}{2}\rangle$ for electrons in the conduction band and $|\pm\frac{3}{2}\rangle$ for holes in the heavy-hole valence band. Therefore, the total exciton spin of heavy-hole excitons can be $|\pm 1\rangle$ or $|\pm 2\rangle$. The latter are optically inactive and cannot be photoexcited. Thus, exciting resonantly the exciton transition with σ^+ or σ^- circularly polarized laser pulses, only $|+1\rangle$ or $|-1\rangle$ excitons are generated, respectively, while for linear polarization of the exciting laser pulse $|+1\rangle$ excitons and $|-1\rangle$ excitons are created equally. As the biexciton state involves two excitons with opposite spin orientations, an exciton spin-flip process is required in the case of circularly polarized excitation in order to form biexcitons, while this process is not required for linearly polarized excitation.

In Fig. 3 the spectrally integrated PL intensity of the biexciton is plotted versus delay time after linearly (stars) and circularly (circles) polarized laser pulses, respectively. The same energy and density of the exciting laser pulse was used in both cases. Excitons are generated resonantly in localized

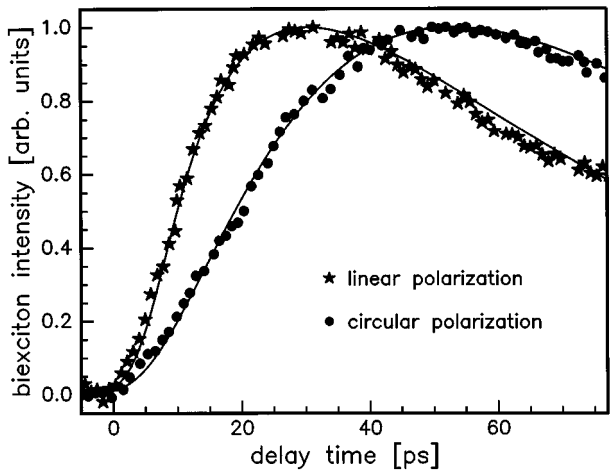

FIG. 3. Normalized PL intensity of the biexciton transition as a function of delay time. Localized excitons with an initial density of about 1×10^9 cm^{-2} have been generated by resonant excitation at the low-energy side of the exciton peak with linearly (stars) and circularly (circles) polarized laser pulses. The solid lines represent theoretical fits according to Eqs. (2)–(4).

states by tuning the wavelength of the exciting laser pulse to the low-energy side of the exciton absorption signal. Thus any further relaxation process except the formation of biexcitons can be excluded. For linear polarization, a fast onset of the biexciton signal reaching the maximum after about 30 ps is observed. In this case, excitons with spin $|+1\rangle$ and $|-1\rangle$ are generated equally. Thus the formation of biexcitons from two excitons with opposite spin orientation determines the rise time of the biexciton luminescence. In contrast, using circularly polarized laser pulses, the rise time of the biexciton signal is significantly increased and the PL signal reaches its maximum about 50 ps after the excitation. In this case excitons with parallel spin orientation are created. As a consequence, a spin-flip process of excitons is required in order to form a biexciton, resulting in an increase of the biexciton rise time. Therefore, we are able to investigate the biexciton formation process as well as the exciton-spin-relaxation rate by analyzing the biexciton transient for the two different excitation conditions described above.

Applying a straightforward kinetic theory, the rate equations under pulsed generation describing a system of interconverting spin-up excitons, spin-down excitons, and biexcitons with densities $X^\uparrow$, $X^\downarrow$, and B, respectively, are

$$\frac{dX^\uparrow}{dt} = -\frac{X^\uparrow}{\tau_X} - \frac{X^\uparrow}{2\tau_U} + \frac{X^\downarrow}{2\tau_U} - CX^\uparrow X^\downarrow + \frac{B}{2\tau_B} + g^\uparrow(t), \quad (2)$$

$$\frac{dX^\downarrow}{dt} = -\frac{X^\downarrow}{\tau_X} - \frac{X^\downarrow}{2\tau_U} + \frac{X^\uparrow}{2\tau_U} - CX^\uparrow X^\downarrow + \frac{B}{2\tau_B} + g^\downarrow(t), \quad (3)$$

$$\frac{dB}{dt} = -\frac{B}{\tau_B} + CX^\uparrow X^\downarrow, \quad (4)$$

where τ_X and τ_B are the exciton and biexciton lifetimes, respectively, τ_U is the exciton spin-flip time, C is the biexciton formation coefficient, and $g^\uparrow(t)$ and $g^\downarrow(t)$ are the δ-like generation rates in the case of pulsed excitation for $X^\uparrow$ and $X^\downarrow$, respectively. The thermal dissociation of biexci-

tons into excitons was neglected in Eqs. (2)–(4), which is a rather good assumption for the low temperature of 2 K and the high biexciton binding energy prevalent in our experiment.

The above rate equations were solved numerically. The resulting time transients of the biexciton luminescence were compared to the experimental data, taking into account the finite-time resolution by convolving the theoretical time transients with the experimentally obtained transient of the laser pulse. The fitting procedure was done as follows. In the first step the biexciton transient obtained after linearly polarized laser excitation was modeled. In this case the exciton-spin-relaxation process does not affect the dynamics of biexcitons, as both spin components are generated equally. The onset of the biexciton signal is determined by the biexciton formation coefficient. In the second step we modeled the biexciton transient obtained after circularly polarized excitation with the same excitation density and excitation energy as in the case of linearly polarized laser pulses. In this part of the fitting procedure the exciton-spin-relaxation time was the only parameter to be varied in order to describe the onset of the biexciton luminescence signal. The exciton and biexciton lifetimes as well as the biexciton formation coefficient were taken from the corresponding linearly polarized experiments. For this reason an accurate determination of the spin-flip time of excitons can be obtained from the numerical analysis of the data.

1. Biexciton formation process

As the formation of biexcitons is a bimolecular process, the increase of the biexciton population is nonexponential and therefore cannot be described by a single time constant. Thus the biexciton formation process is characterized by the biexciton formation coefficient. In order to obtain the biexciton formation coefficient, the exciton peak density generated by the laser pulse has to be determined accurately. The corresponding value was estimated from the peak power, the focus, and the width of the laser pulse, taking into account reflective losses of the incident power at the focusing lens, the cryostate windows, and the sample surface. An absorption coefficient of $\alpha = 1 \times 10^5$ cm^{-1} at the maximum of the excitonic absorption[23] was used. The energy dependence of the absorption coefficient was considered by varying the exciting laser power according to the absorption profile in order to obtain an initial exciton density independent of the excitation energy.

In Fig. 4 the biexciton formation coefficient C as derived from the experiments with linearly polarized laser excitation is plotted as a function of the excitation energy (squares) for an initial exciton density of 1×10^9 cm^{-2}. For comparison, the PL spectrum (dashed line) showing the exciton (X) and the biexciton (B) luminescence and the photoluminescence excitation (PLE) spectrum (solid line) showing the absorption peak of the heavy-hole exciton are included in the figure. The Stokes shift of about 3 meV between the absorption peak and the luminescence of the heavy-hole exciton indicates the influence of localization effects due to alloy and/or well width fluctuations in this ternary (Zn,Cd)Se/ZnSe quantum-well system.

For the lowest excitation energy, i.e., resonant excitation of excitons in localized states, the biexciton formation coefficient is about 5.2×10^{-11} cm^2/ps. Increasing the excitation energy, the biexciton formation coefficient decreases. A value of about 1×10^{-11} cm^2/ps is obtained for excitation at the high-energy side of the excitonic absorption ($E = 2.688$ eV). From these results we conclude that the biexciton formation from localized excitons seems to be much more efficient than from mobile ones. This is in qualitative agreement with results obtained for GaAs quantum wells.[24,25] They have shown that the biexciton formation is drastically enhanced for a resonant generation of cold excitons compared to nonresonant excitation. This was associated with the presence of excess translational energy in the latter case. However, a detailed energy dependence of the biexciton formation efficiency was not shown.

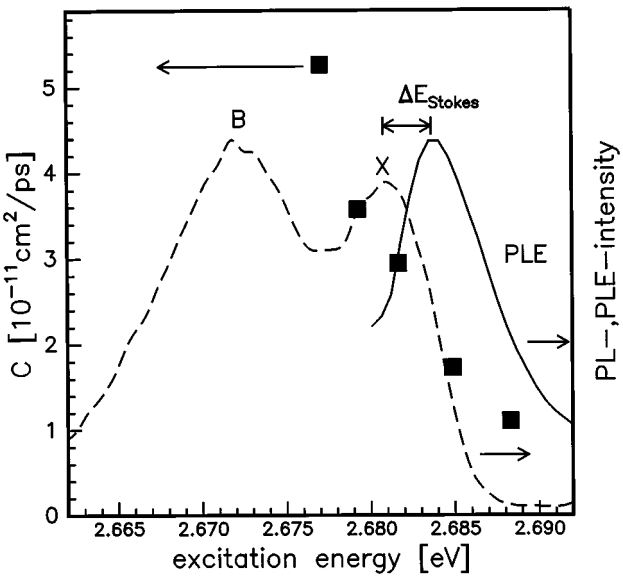

FIG. 4. Dependence of the biexciton formation coefficient on excitation energy for an initial carrier density of 1×10^9 cm^{-2} (full squares). The dashed and the solid line represent the PL and the PLE spectrum of the corresponding quantum well, respectively. The Stokes shift ΔE_{Stokes} between the PL and the PLE signal amounts to about 3 meV.

2. Spin-flip processes of excitons

In Fig. 5(a) the exciton-spin-relaxation time τ_U (full circles) obtained from the experiments using circularly polarized laser pulses is plotted versus the excitation energy for an initial exciton density of 1×10^9 cm^{-2}. Additionally, the PL (dotted line) and the PLE spectrum (dashed line) of the quantum well are shown. For resonant excitation of excitons in localized states ($E = 2.677$ eV), the exciton-spin-relaxation time τ_U is about 70 ps and decreases to a value of about 20 ps as the excitation energy is tuned across the exciton peak to 2.688 eV. This demonstrates an enhanced spin-flip rate for delocalized excitons as compared to localized ones.

To evaluate the responsible spin-flip mechanism of excitons, the square of the exciton-spin-relaxation rate $R = 1/\tau_U$ is plotted in Fig. 5(b) as a function of excitation energy. Adreani and Bassani have shown that the long-range exchange interaction for heavy-hole excitons in a quantum well vanishes linearly with the wave vector K.[26] The solid line in

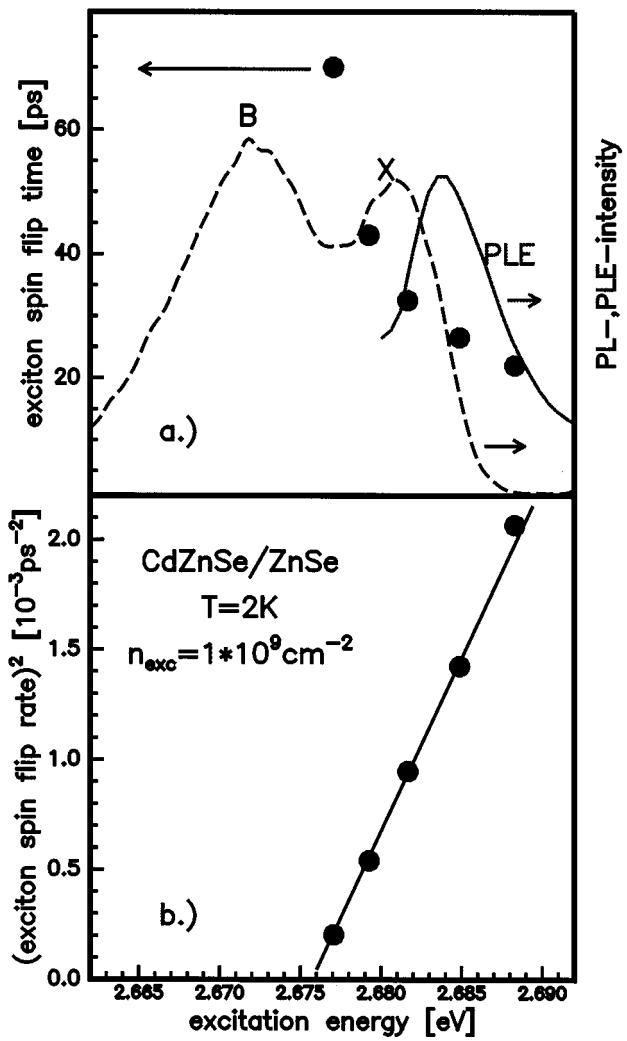

FIG. 5. (a) Exciton spin relaxation time and (b) square of the exciton spin relaxation rate as a function of excitation energy for an initial carrier density of 1×10^9 cm^{-2}. In (a), the dashed and the solid line represent the PL and the PLE spectrum of the corresponding quantum well, respectively. In (b), the solid line is a fit to the data as described in the text.

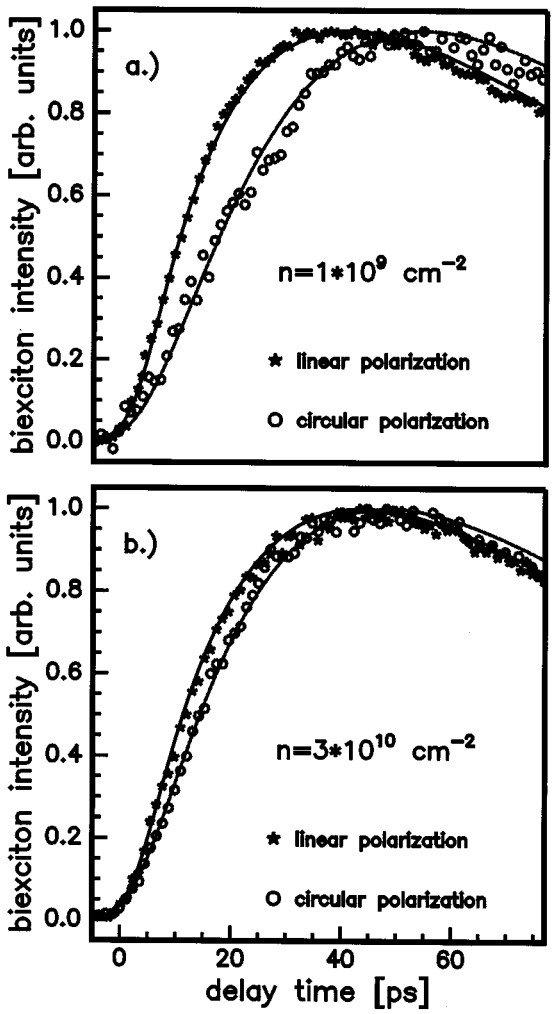

FIG. 6. Normalized PL intensity of the biexciton transition as a function of delay time for an excitation energy $E=2.682$ eV with linearly (stars) and circularly (circles) polarized laser pulses for an initial carrier density of (a) 1×10^9 cm^{-2} and (b) 3×10^{10} cm^{-2}.

Fig. 5(b) representing the dependence $R^2\propto E(\propto K^2)$ therefore indicates that the long-range exchange interaction seems to be the spin-flip mechanism responsible for the excitons in the investigated quantum-well structure.

In Fig. 6 the spectrally integrated intensity of the biexciton signal is plotted versus delay time after linearly (stars) and circularly (circles) polarized laser excitation at 2.682 eV (i.e., the maximum of the excitonic luminescence peak). The initial carrier density was $n_{ex}=1\times10^9$ cm^{-2} [Fig. 6(a)] and $n_{ex}=3\times10^{10}$ cm^{-2} [Fig. 6(b)]. The difference of the biexciton onset after linearly and circularly polarized excitation, which is mainly controlled by the time constant required for the exciton spin-flip process, is reduced drastically with increasing excitation density. From a quantitative description of the experimental data using the model described above (solid lines), a decrease of the exciton spin-flip time from about 35 ps at $n_{ex}=1\times10^9$ cm^{-2} to about 15 ps at $n_{ex}=3\times10^{10}$ cm^{-2} was obtained.

A similar behavior was observed by Muñoz *et al.* in GaAs quantum wells.[14] The faster spin relaxation at high excitation densities was explained by the proportionality of the spin-relaxation time and the inverse carrier momentum relaxation time according to either the D'yakonov-Perel' mechanism[27] or the exchange interaction. At low temperatures the carrier momentum relaxation may be determined by scattering with residual ionized impurities[28] and a higher carrier density will screen the Coulombic interaction with the charged impurities.[29] Thus an increase of the carrier concentration results in a higher carrier mobility, i.e., longer carrier momentum relaxation time due to screening. Therefore, a shorter spin-relaxation time is expected.

On the other hand, an increase of the excitation density causes a filling of the localized states and the successive occupation of free-exciton states. As free excitons are characterized by a faster spin-flip time than localized ones [see Fig. 5(a)], an increase of the laser intensity would result in a faster exciton-spin relaxation process. However, from our

experiments, it is not possible to separate one of the two mechanisms described above.

IV. CONCLUSION

In summary, time-resolved and time-integrated photoluminescence spectroscopy have been performed in order to gain insight into the biexciton formation process and the dynamics of exciton-spin relaxation in (Zn,Cd)Se/ZnSe quantum wells. By adjusting the polarization of the exciting laser pulse, a well-defined spin state of the generated exciton gas was established. Direct access to the relevant time constants have been obtained by analyzing quantitatively the time evolution of the biexciton signal for various excitation conditions. The experimental data demonstrate the importance of localization effects for a quantitative understanding of the exciton and the biexciton dynamics. Generating resonantly localized excitons, we obtain a biexciton formation coefficient of about 5.2×10^{-11} cm^2/ps and a spin-flip time of excitons of 70 ps. Creating mobile excitons, both the biexciton formation coefficient and the exciton spin-flip time significantly decrease. This indicates, on the one hand, a less efficient formation of biexcitons from free excitons than from mobile ones. On the other hand, we conclude from the energy dependence of the exciton-spin flip rate that the long-range exchange interaction is most likely the dominating mechanism controlling the low-temperature spin dynamics in (Zn,Cd)Se/ZnSe quantum wells.

ACKNOWLEDGMENT

We gratefully acknowledge the financial support of this work by the Deutsche Forschungsgemeinschaft (Grant No. SFB410).

*Present address: Institut für Festkörperphysik, Universität Bremen, P. O. Box 330440, D-28334 Bremen, Germany.

[1] N. Pelekanos, J. Ding, A. V. Nurmikko, H. Luo, N. Samarth, and J. K. Furdyna, Phys. Rev. B **45**, 6037 (1992).
[2] Q. Fu, D. Lee, A. Mysyrowicz, and A.V. Nurmikko, Phys. Rev. B **37**, 8791 (1988).
[3] Y. Yamada, T. Mishina, Y. Masumoto, Y. Kawakami, S. Yamaguchi, K. Ichino, S. Fujita, and T. Taguchi, Phys. Rev. B **51**, 2596 (1995).
[4] J. Suda, Y. Kawakami, S. Fujita, and S. Fujita, Jpn. J. Appl. Phys. **33**, L986 (1994).
[5] U. Neukirch, D. Weckendrup, J. Gutowski, D. Hommel, and G. Landwehr, J. Cryst. Growth **138**, 861 (1994).
[6] F. Kreller, M. Lowisch, J. Puls, and F. Henneberger, Phys. Rev. Lett. **75**, 2420 (1995).
[7] H. Grempel, A. Diessel, W. Ebeling, J. Gutowski, K. Schüll, B. Jobst, D. Hommel, M.F. Pereira, Jr., and K. Henneberger, Phys. Status Solidi B **194**, 199 (1996).
[8] Li Wang and J.H. Simmons, Appl. Phys. Lett. **67**, 1450 (1995).
[9] J. Puls, H.J. Wünsche, and F. Henneberger, J. Chem. Phys. (to be published).
[10] J. Puls, V.V. Rossin, F. Kreller, H.J. Wünsche, St. Renisch, N. Hoffmann, M. Rabe, and F. Henneberger, J. Cryst. Growth **159**, 784 (1996).
[11] D.S. Citrin, Phys. Rev. B **50**, 17 655 (1994).
[12] J.C. Kim, D.R. Wake, and J.P. Wolfe, Phys. Rev. B **50**, 15 099 (1994).
[13] S. Charbonneau, T. Steiner, M.L.W. Thewalt, E.S. Koteles, J.Y. Chi, and B. Elman, Phys. Rev. B **38**, 3583 (1988).
[14] L. Muñoz, E. Pérez, L. Viña, and K. Ploog, Phys. Rev. B **51**, 4247 (1995).
[15] T.C. Damen, L. Viña, J.E. Cunningham, J. Shah, and L.J. Sham, Phys. Rev. Lett. **67**, 3432 (1991).
[16] S. Bar-Ad and I. Bar-Joseph, Phys. Rev. Lett. **68**, 349 (1992).
[17] T.C. Damen, K. Leo, J. Shah, and J.E. Cunningham, Appl. Phys. Lett. **58**, 1902 (1991).
[18] M.Z. Maialle, E. A. de Andrada e Silva, and L.J. Sham, Phys. Rev. B **47**, 15 776 (1993).
[19] L.J. Sham, J. Phys. Condens. Matter **5**, A51 (1993).
[20] M.R. Freeman, D.D. Awschalom, J.M. Hong, and L.L. Chang, Phys. Rev. Lett. **64**, 2430 (1990).
[21] G. Bacher, M. Illing, A. Forchel, D. Hommel, B. Jobst, and G. Landwehr, Phys. Status Solidi B **187**, 371 (1995).
[22] P.L. Gourley and J.P. Wolfe, Phys. Rev. B **25**, 6338 (1982).
[23] J. Ding, N. Pelekanos, A.V. Nurmikko, H. Luo, N. Samarth, and J.K. Furdyna, Appl. Phys. Lett. **57**, 2885 (1990).
[24] R.T. Phillips, D.J. Lovering, G.J. Denton, and G.W. Smith, Phys. Rev. B **45**, 4308 (1992).
[25] D.J. Lovering, R.T. Phillips, G.J. Denton, and G.W. Smith, Phys. Rev. Lett. **68**, 1880 (1992).
[26] L.C. Adreani and F. Bassani, Phys. Rev. B **41**, 7536 (1990).
[27] M.I. D'yakonov and V.I. Perel', Zh. Éksp. Teor. Fiz. **60**, 1954 (1971) [Sov. Phys. JETP **33**, 1053 (1971)].
[28] J.C.M. Hwang, A. Kastalsky, H.L. Stormer, and V.G. Keramidas, Appl. Phys. Lett. **44**, 639 (1984).
[29] G. Bastard, *Wave Mechanics Applied to Semicondutor Heterostructures* (Wiley, New York, 1991).